

A NOVEL APPROACH FOR RADAR DETECTION OF HIGH SPEED SMALL TARGETS WITH CFAR ALGORITHM

Dr. Habibullah Khan*, B. Sree deepthi**

* (Professor, Department of ECE, K L University, Vaddeswaram)

** (M.tech student, Department of ECE, K L University, Vaddeswaram)

ABSTRACT

Detection, parameter extraction and the tracking of moving high speed small targets are challenging tasks for the radar system design and in most of radar applications, target's range migration was one of the reasons that limits integration time and consequently reduces the processing gain. The high speed makes the target shift through range cells during the observation period, making it difficult to improve the target's reflecting energy, coherent accumulation and the signal-to-noise ratio. In this paper, an efficient and accurate range-cell migration correction method with very low computation burden through shifting control on the matching weight coefficients is used and then spatial-temporal cell averaging constant false alarm rate algorithm is used for the detection of moving high speed small targets in presence of heavy clutter and noise.

Keywords –RLOS, MEI, Range walk, Cross-range, CFAR.

I. INTRODUCTION

In most of the radar applications, like target sensing (detection, location, tracking, viewing, and identification), the relative velocity measurement, navigation, weather avoidance, ground mapping, terrain avoidance and weapon delivery, the main objective is to detect targets of interest while estimating each target's position and velocity. A small target appears as a point target in narrowband radar and occupies only one range cell with small reflectivity, which makes the target detection difficult. To improve the radar detection capability, a long coherent observation time is required. For space targets, velocity along the radar line-of-sight (RLOS) is much higher than the conventional target^[14], which makes the target migrate through different range cells with unknown Doppler frequency in the long observation period. Therefore, the target echo cannot be coherently accumulated in its observation period, which is vital for small target detection. Some compensation

methods are presented for small target detection in^[1–3], such as keystone transform, range stretching and joint time frequency processing, and matched Fourier transform (MFT). A spectral matching approach is developed for narrowband signal detection in^[4] by using a priori knowledge of the signal power spectral density (PSD). In^[5], a narrowband radar detection algorithm for weak signals with long duration time and unknown frequency structure is investigated. In^[6–8], some higher order statistic (HOS) methods are applied for signal detection. In^[9], a detection method using Gabor's expansion is proposed. In^[10], wavelets are applied to narrowband signal detection. In^[11], weak signal detection in some specific additive noise is considered. In^{[12]–[14]}, only a single pulse is utilized for the target detection.

In this paper, an efficient and accurate range-cell migration correction method is used for estimation. And the discussion is based on the hypotheses: (1) The velocity of the target is constant during the coherent processing interval (CPI); (2) The range migration in a CPI is larger than the width of the pulse compression output, but far smaller than the width of the transmitted chirp pulse. After that spatial-temporal cell averaging constant false alarm rate algorithm is used for the detection of moving targets in presence of heavy clutter and noise.

II. SIGNAL MODEL OF TARGET

Range migration is an unavoidable problem in the tracking of moving targets or long time coherent integration. The range walk mainly occurs due to the target velocity and acceleration. The echo signal characteristic of a chirp pulse train from a moving target is analyzed at first. It is pointed out that the range migration is caused by the migration exponential item (MEI) of the echo signal and can be compensated by removing the MEI before the processing of match filtering and coherent integration.

The effect on the radar electromagnetic wave due to the motion of a target presents the echo signal time scale change (time stretching or shrinking).

Assume that the transmitted signal is $s(t)$, then the echo from a moving target with velocity radial velocity v can be expressed as :

$$S_r(t) = \eta S(k(t-t_0)) \quad (1)$$

Where η is the amplitude of the echo signal (here it was assumed $\eta = 1$); $t_0 = 2R_0/(c+v)$ is the delay of the wave front; c is the velocity of light; and R_0 is the original distance of the target. k is the compressing coefficient.

$$k = (c + v)/(c - v) \quad (2)$$

When transmitting a chirp pulse train, $S(t)$ can be expressed by

$$S(t) = \sum_{m=0}^{M-1} u(t - mT) e^{j2\pi f_c t} \quad (3)$$

here, M is the amount of pulse burst; T denotes the PRI; f_c represents the carrier frequency; and

$$u(t) = \text{rect}\left(\frac{t}{T_p}\right) e^{j\frac{1}{2}\mu t^2} \quad (4)$$

is the chirp signal; μ is modulation rate; and T_p denotes the width of the pulse. And

$$\text{rect}\left(\frac{t}{T_p}\right) = \begin{cases} 1 & 0 \leq t \leq T_p \\ 0 & \text{else} \end{cases} \quad (5)$$

According to equations (1) and (3), the received signal can be expressed as:

$$S_r(t) = \sum_{m=0}^{M-1} u(k(t - t_0) - mT) e^{j2\pi f_c (k(t-t_0))} \quad (6)$$

After mixing with the local oscillator signal, the output base band signal is :

$$S_{r_I}(t) = \sum_{m=0}^{M-1} u(k(t - t_0) - mT) e^{j2\pi f_d t} e^{-j\phi} \quad (7)$$

Where $f_d = 2vf_c/(c - v)$ is the Doppler frequency, and $\phi = 2\pi f_c t_0$ is the initial phase of the echo signal. Denote t as:

$$t = \hat{t} + mT \quad (8)$$

Where \hat{t} is the “fast time” in a PRI, and m represents the “slow time” for different period. For simplification, we supposed that $t_0 \in [0, T]$. Then the base band signal $s_{r_I}(t)$ can be expressed as a bi dimensional form:

$$S_{r_I}(\hat{t}, m) = u[k(\hat{t} - t_0) + (k - 1)mT] e^{j2\pi f_d (\hat{t} + mT)} e^{-j\phi} \quad (9)$$

Define migration factor k_v :

$$k_v = k - 1 = 2v/c - v \quad (10)$$

k_v represents the relative amount of migration between adjacent PRIs. According to equations (4) and (10), (9) can be expanded as:

$$S_{r_I}(\hat{t}, m) = \text{rect}\left(\frac{k(\hat{t} - t_0) + k_v mT}{T_p}\right)$$

$$\cdot e^{j\frac{1}{2}\mu (k(\hat{t} - t_0) + k_v mT)^2} \cdot e^{j2\pi f_d (\hat{t} + mT)} \cdot e^{-j\phi}$$

$$S_{r_I}(\hat{t}, m) = \text{rect}\left(\frac{k(\hat{t} - t_0) + k_v mT}{T_p}\right)$$

$$\cdot e^{j\frac{1}{2}\mu (k(\hat{t} - t_0))^2} \cdot e^{j2\pi f_d \hat{t}} \cdot e^{j\frac{1}{2}\mu [(k_v mT)^2 - 2k t_0 k_v mT]}$$

$$\cdot e^{j2\pi f_d mT} \cdot e^{j\mu k t_0 k_v mT} \cdot e^{-j\phi} \quad (11)$$

Define :

$$u_1 = e^{j\frac{1}{2}\mu (k(\hat{t} - t_0))^2} \cdot e^{j2\pi f_d \hat{t}} \quad (12)$$

$$u_2 = e^{j\frac{1}{2}\mu (k_v mT)^2} \cdot e^{j2\pi f_d mT} \cdot e^{-j\mu k t_0 k_v mT} \quad (13)$$

$$u_3 = e^{j\mu k t_0 k_v mT} \quad (14)$$

The total migration in a CPI is $k_v MT = 2vMT/(c - v)$, which is far smaller than the width T_p of the chirp pulse before compressed, and so

$$\text{rect}\left(\frac{k(\hat{t} - t_0) + k_v mT}{T_p}\right) \approx \text{rect}\left(\frac{\hat{t} - t_0}{T_p}\right) \quad (15)$$

$$S_{r_I}(t, m) = \text{rect}\left(\frac{(t - t_0)}{t_p}\right) \cdot u_1 u_2 u_3 \cdot e^{-j\phi} \quad (16)$$

III. ANALYSIS OF THE MEI

$U_1(\dot{t})$ is the common item of single chirp pulse echo from a moving target, which can be processed by ordinary match filtering. $U_2(m)$ is a function of slow time m . It can be written as

$$U_2(m) = U_{21}(m)U_{22}(m)U_{23}(m) \quad (17)$$

Where, $U_{23}(m) e^{j2\pi f_d m T}$ is the normal element caused by Doppler frequency, and $U_{21}(m) = e^{j\frac{1}{2}\mu(k_v m T)^2}$ is an extra chirp component in the slow time, which will widen the Doppler bandwidth slightly. $U_{22}(m) = e^{-j\mu k t_0 k_v m T}$ is a sine wave, whose frequency is determined by t_0 , and U_{22} may change the Doppler frequency of the target, but it does not influence the coherent integration.

Notice that U_1 and U_2 have nothing to do with the range migration, and $U_3 = e^{j\mu k t_0 k_v m T}$ is related not only to the fast time \dot{t} , but also to the slow time m . Thereby, U_3 is the determinant of range migration and coherent integration loss. So we call U_3 migration exponential item (MEI).

When tracking slow targets with narrowband signal, we have $k_v \approx 0$, so $U_3 \approx 1$, $U_{21} \approx 1$, $U_{22} \approx 1$, and

$$S_{r_I}(t, m) \approx \text{rect}\left(\frac{(t - t_0)}{t_p}\right) \cdot e^{j\frac{1}{2}\mu(k(k - t_0))^2} \cdot e^{j2\pi f_d \dot{t}} \cdot e^{j2\pi f_d m T} \cdot e^{-j\phi} \quad (18)$$

The processing in the fast and slow times are mutually independent. The ordinary method is match filtering in the fast time and coherent integration using FFT algorithm in the slow time. As the signal bandwidth is much wider and the target velocity is much higher, the migration factor k_v becomes greater, and the range migration across pulse repetition period cannot be ignored. The loss of gain in coherent integration arising from MEI must be taken into account. Since U_3 is the determinant of range migration, we can eliminate range migration by remove the MEI. And this can be achieved by multiplying $S_{r_I}(t, m)$ with $e^{-j\mu k t_0 k_v m T}$.

$$S_{r_{IOUT}}(t, m) = S_{r_I}(t, m) \cdot e^{-j\mu k t_0 k_v m T} \quad (19)$$

The above operation results in the change of Doppler frequency shift in each PRI, which then leads to the

complementary migration of the signal envelope. The new signal matrix $S_{r_{IOUT}}(t, m)$ then can be processed with the ordinary method.

IV. RANGE MIGRATION COMPENSATION BASED ON SHIFTING THE MATCHING WEIGHT COEFFICIENTS

As shown above, the range migration can be compensated by removing the MEI. This method is essentially based on the Doppler-range relationship of chirp signal, and it does not produce any parasitic side lobes in the output as long as the compensation is accurate. In this section, we will introduce a new practical method with low additional computation burden and low processing complexity. The matched filtering of chirp signal can be completed in the frequency domain by means of Fast Fourier Transform (FFT), and the implementary scheme is shown in Fig. 1. The matching weight is the spectrum of the local chirp signal, which can be calculated beforehand by FFT and stored in the storage of the processing system.

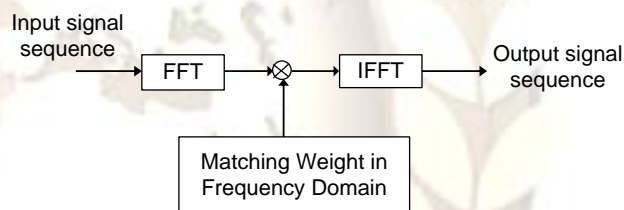


Figure 1: Digital match filtering performed in frequency domain.

The matching weight coefficients can be expressed as

$$U(k) = \text{DFT}(u^*(-n)) = \sum_{n=0}^{N-1} u^*(-n) e^{-j\frac{2\pi}{N}nk} \quad (20)$$

Where $k = 0, 1, \dots, N - 1$.

Where $*$ denotes conjugation operation; $u^*(-n) = u^*(-nT_s)$ is the samples of local chirp signal $u^*(-t)$ with sampling period T_s ; and N is the length of the sequence.

A. Description of the Method Based on Shifting the Matching Weight Coefficients

In order to compensate the range migration between different pulse repetition periods, different matching signals should be used:

$$v(t) = u(t)e^{-j2\pi f_b(m)t} \quad (21)$$

Where $f_b(m)$ is the introduced frequency component in different periods for revising the envelope position of the matched filtering output, the output signal of match filtering can be expressed as:

$$y(\hat{t}, m) = S_{r1}(\hat{t}, m) \otimes v^*(-t) \\ = \left\{ u^*(-t) \otimes \text{rect}\left(\frac{\hat{t}-t_0}{T_P}\right) \right\} \cdot U_2 \cdot e^{-j\Phi} \\ \cdot U_1 \cdot U_3 \cdot e^{-j2\pi f_b(m)t} \quad (22)$$

Where \otimes denotes convolution integration. The condition under which the envelope position of $y(\hat{t}, m)$ is independent of m is

$$f_b(m) = \frac{1}{2\pi} m \mu k k_v T + f_{d0} \quad (23)$$

Here, $\frac{1}{2\pi} m \mu k k_v T$ is exactly the frequency item of the MEI. f_{d0} is the initial Doppler frequency, which could be determined by prior information about the target velocity. f_{d0} has no direct effect on the envelope migration, but it will influence the estimation precision of target distance.

It is impossible to storage all potential weight coefficients corresponding to different $f_b(m)$. If we quantize $f_b(m)$ with $1/NT_s$, then it can be written as:

$$f_b(m) = \frac{k_b}{NT_s} \quad (24)$$

Where $k_b = 0, 1, \dots, M-1$.

Formula (24) is an approximate expression of the quantized result. Then $v(t)$ can be expressed as:

$$v(t) = u(t)e^{-j\frac{2\pi}{NT_s}k_b t} \quad (25)$$

According to equation (20), we have

$$U(k) = DFT(u^*(-n)) = \sum_{n=0}^{N-1} u^*(-n)e^{-j\frac{2\pi}{N}n(k+k_b)} \quad (26)$$

Therefore, $V(k)$ can be obtained by shifting $U(k)$, and doesn't need to be stored in addition. So we get the method of range migration compensation by shifting the matching weight coefficients, as shown in Fig. 2.

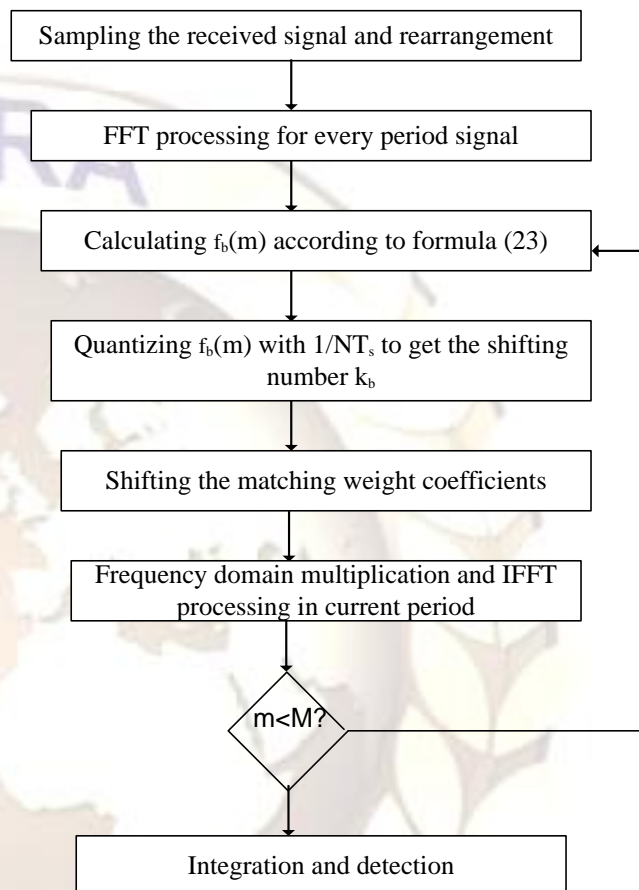


Figure 2: Long time coherent integration with migration compensation by shifting the matching weight coefficients.

This method only appends a few division and shifting operations to the ordinary matching processing, so the additional computation burden is very limited.

B. Parasitic Side lobes and Restraining Method:

There exists quantization error when using $1/NT_s$ to quantize $f_b(m)$. It results in parasitic side lobes produced in the Doppler domain. This is because the envelopes of the matched filtering output are aligned approximatively, and

periodic amplitude modulation to the output in the slow time domain is produced. The position and amplitude of the parasitic side lobes are related to the velocity of the target. This kind of parasitic side lobe also exists in the range-bin realignment algorithm and the envelope interpolation algorithm. The effectual method to restrain the parasitic side lobe is to reduce the quantization error. When the sequence length and the sampling period are determined, we can store multi groups of weight to reduce the quantization error of $f_b(m)$. Suppose there are L groups of weight, the l^{th} group of weight coefficients can be wrote as:

$$V_l(k) = \sum_{n=0}^{N-1} v^*(-n) e^{-j\frac{2\pi}{N}n(k+l/L)} \quad (27)$$

Where, $l = 0, 1, \dots, L - 1$

Thus, the quantized interval can be turned into $1/LNT_s$, which is much smaller than the frequency interval of the matching weight coefficients. Therefore, we should modify the processing flow of long time coherent integration.

Compared with the ordinary algorithm, the above algorithm in Fig. 3 needs much more storage space, which is not the vital bottleneck in signal processing because of the hyper growth of the digital technique. In practical use, it can get a balance between the hardware expense and the processing performance.

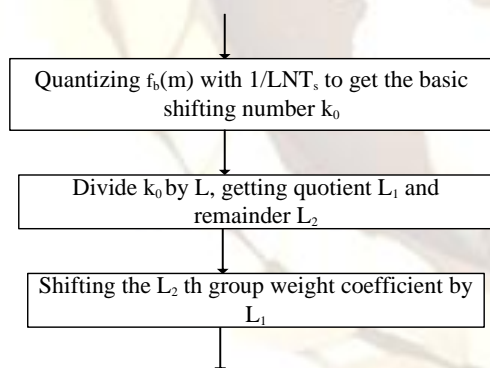


Figure 3: Choosing and shifting control of the matching weight coefficients when storing multi-groups of weight.

V. CFAR ALGORITHM

The signal returns from radar targets are usually buried in thermal noise and clutter. So a proper threshold level is to be known to detect the targets, which can be accomplished by constant false alarm rate (CFAR) algorithm. Since neither the clutter power nor

the noise power is known at any given location, a fixed threshold detection processor cannot be applied if the false alarm rate is desired to be controlled. Therefore, it is necessary for automatic detection of targets for radars applications to be adaptive to variations in background clutter in order to achieve the CFAR property. The CFAR detector is one of the most important parts of modern radar signal processing. It can be used to avoid computer overloading, which is caused by radar clutter fluctuation, and obtain high detection performance.

For complex environment such as anti-collision automotive radars, where the environment changes abruptly, these conventional detectors cannot detect targets properly. With the use of a modified CFAR concept, it would meet the mentioned requirements concerning detection probability, false alarm rate and low computation complexity. Two major problems that require careful investigation in such a CFAR detection scheme are those presented by 1) regions of clutter power transition and by 2) multiple target environments. The first situation occurs when the total noise power received within a single reference window changes abruptly. The presence of such a clutter edge may result in severe performance degradation in an adaptive threshold scheme leading to excessive false alarms or serious target masking depending upon whether the cell under test is a sample from clutter background or from relatively clear background with target return, respectively. The second situation is encountered when there are two or more closely spaced targets in range. The interfering targets that appear in the reference window along with the target under investigation (known as primary target) may raise the threshold unnecessarily. Often a CFAR detector only reports the stronger of the two targets.

The early CFAR detector called cell-averaging CFAR (CA-CFAR) was proposed by Finn and Johnson. In this detector, the adaptive threshold is the arithmetic mean of its reference cells. Many CFAR algorithms are developed to meet different situations namely in a transition in the clutter power distribution and the presence of interfering targets which refer to targets present in the reference window cells. When the number of interfering targets exceeds the supposed one, the developed detectors exhibit a serious performance degradation. This CFAR is best suits for homogeneous environments. In non-homogeneous environments, clutter map (scan-by-scan) processing is deployed. The performance of this method degrades in the presence of slow targets. In this paper, a hybrid procedure for CFAR is proposed, which combines the advantages of both spatial and time averaging. And the detailed description of spatial-

temporal cell averaging CFAR algorithm is explained as follows :

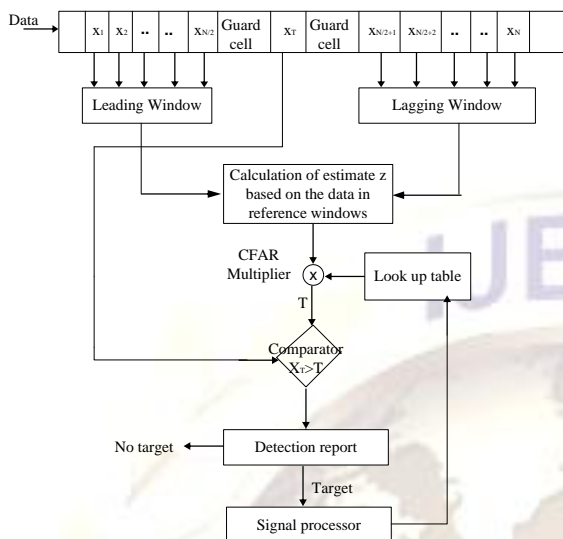


Figure 4: Block diagram of CA-CFAR algorithm.

CA-CFAR processor consists of window of length $N+1$. Where N is number of cell surrounding the Cell Under Test (CUT). Processing of CUT, leading and lagging windows produce an estimate Z which is later used to target detection. We assume that output for any range cell is exponentially distributed with Probability Density Function (PDF) given by

$$f(x) = \frac{1}{2\lambda} e^{-\frac{x}{2\lambda}} \quad x \geq 0 \quad (28)$$

Where λ is the total background clutter plus thermal noise power given as μ under the null hypothesis H_0 and λ is defined as $\mu(1+S)$ where S is the average signal to noise ratio(SNR) of a target. The PFA is given by

$$PFA = P[Y > Y_0 | H_0] = e^{-\frac{Y_0}{2\mu}} \quad (29)$$

Where Y_0 denotes the fixed optimum threshold. Similarly the optimum detection probability PD is given by

$$PD = P[Y > Y_0 | H_1] = e^{-\frac{Y_0}{2\mu(1+S)}} \quad (30)$$

The below figure shows the structure of clutter map constant false alarm rate. A clutter map divides the radar coverage area into cells on polar or rectangular

grid. The clutter echo stored in each cell of the map can be used to establish threshold, it is then a form of CFAR. The size of each clutter map cell is equal or greater than radar resolution.

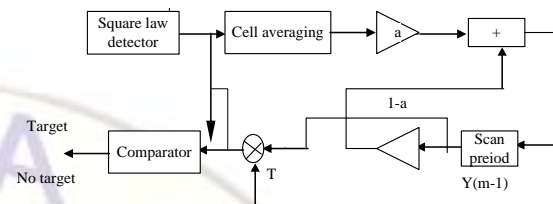


Figure 5 : Block diagram of the spatial-temporal cell averaging-CFAR algorithm.

Clutter magnitude is estimated as:

$$Y(0)=X(0) \quad (31)$$

$$Y(m)=(1-a)Y(m-1)+aX(m) \quad (32)$$

Where $Y(m)$ is estimated clutter value after m scans, a is a clutter map gain and $X(m)$ is clutter map update value.

Assuming that there are M resolution cells ($x(1,j) \dots x(M,j)$) in clutter map cell their average clutter level is calculated as:

$$X(m) = \sum_{i=1}^M x(i, m) \quad (33)$$

Where value of j denotes order of the resolution cell in the clutter map cell. We can rewrite equation (33) into the general form as:

$$Y(m) = \sum_{n=1}^m h(n - m)X(n) \quad (34)$$

$$h(n) = \begin{cases} a(1-a)^n & 0 \leq n \leq m-1 \\ (1-a)^m & n = m \end{cases} \quad (35)$$

For a given P_{fa} the scaling factor T can be obtained by solving the equation:

$$P_{fa} = \left(\frac{1}{1 + \frac{T(1-a)^m}{M}} \right)^M \prod_{n=1}^m \left(\frac{1}{1 + \frac{T(1-a)^{m-n}}{M}} \right)^M \quad (36)$$

And the detection decision in case of CM-CFAR can be expressed as:

$$D(Y) = \begin{cases} 1 & x(m) \geq T.X(m-1) \\ 0 & x(m) < T.X(m-1) \end{cases} \quad (37)$$

Where value T is a factor for selection of desired constant false alarm rate and the value of x(m) is tested radar echo similar to variable Y.

Assuming a square-law detector, Gaussian noise and Swerling II model for target, the relations between false alarm probability and detection probability in optimum case are

$$P_{fa} = P[y > y_0 | H_0] = \int_{y_0}^{\infty} \frac{1}{2\mu} * e^{(-\frac{x}{2\mu})} dx = e^{(-\frac{y_0}{2\mu})} \quad (38)$$

$$P_d = P[y > y_0 | H_1] = \int_{y_0}^{\infty} \frac{1}{2\mu} * e^{(-\frac{x}{2\mu(1+S)})} dx = e^{(-\frac{y_0}{2\mu(1+S)})} \quad (39)$$

Where y_0 is threshold, μ is noise power for each cell, and S is target signal to noise power ratio. H_1 and H_0 represent hypotheses relating to the presence or absence of target respectively. In the CFAR processor, these probabilities are computed on a window, and are then averaged on the probability density of Z, the random variable of reference samples over all windows. In the complex method presented here, Z is composed of two random variables, z_1 and z_2 , which are the samples that participate in spatial and temporal CFAR respectively. Therefore the detection and false alarm probability functions are

$$\begin{aligned} P_{fa} &= E_{z_1, z_2} \{P[y > (\alpha cz_1 + \beta kz_2) | H_0]\} \\ &= E_{z_1, z_2} \left\{ \int_{\alpha cz_1 + \beta kz_2}^{\infty} \frac{1}{2\mu} e^{(-\frac{y}{2\mu})} dy \right\} \\ &= E_{z_1, z_2} \left\{ e^{(-\frac{\alpha cz_1 + \beta kz_2}{2\mu})} \right\} \end{aligned} \quad (40)$$

Similarly, the detection probability is given by

$$\begin{aligned} P_{fa} &= E_{z_1, z_2} \{P[y > (\alpha cz_1 + \beta kz_2) | H_1]\} \\ &= M_{z_1} \left\{ \frac{\alpha c}{2\mu(1+S)} \right\} * M_{z_2} \left\{ \frac{\beta k}{2\mu(1+S)} \right\} \end{aligned} \quad (41)$$

Applying the above equations for CA-CFAR processor then,

$$M_{z_1}(u) = \left(1 + 2\mu \frac{u}{N}\right)^{-N} \quad (42)$$

Where N is the number of cells that are used in the estimation. For CM-CFAR

$$M_{z_2}(u) = \prod_{i=0}^{\infty} [1 + 2\mu u w (1-w)^i]^{-1} \quad (43)$$

The equations for false alarm and detection probability are thus becomes

$$P_{fa} = \left\{ \prod_{i=0}^{\infty} [1 + \alpha c w (1-w)^i]^{-1} \right\} * \left(1 + \frac{\beta k}{N}\right)^{-N} \quad (44)$$

$$P_d = \left\{ \prod_{i=0}^{\infty} \left[1 + \frac{\alpha c w}{1+s} (1-w)^i\right]^{-1} \right\} * \left(1 + \frac{\beta k}{N(1+s)}\right)^{-N} \quad (45)$$

VI. SIMULATION RESULTS

Obtained equations and values are simulated using the MATLAB software, taking corresponding dimensions on y label and values on x label and graph is plotted by considering different values in different scenarios.

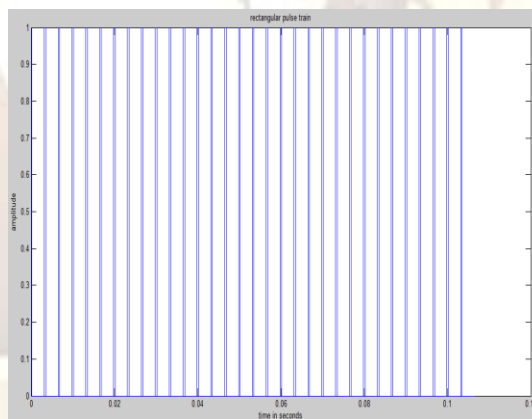


Figure 6: Rectangular pulse train showing 32 pulses.

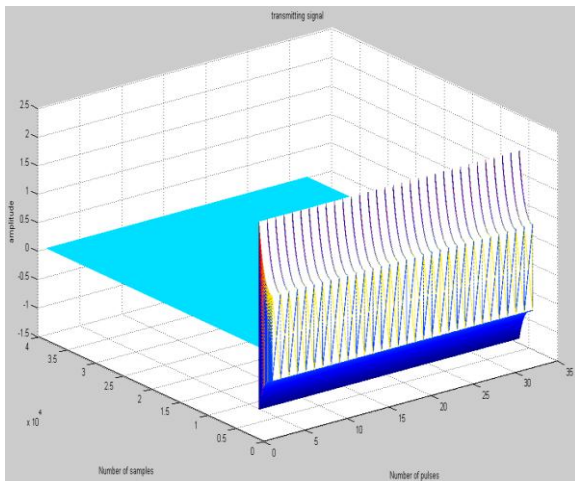


Figure 7 : Transmitted linear frequency modulated (LFM) signal from the radar containing 32 pulses.

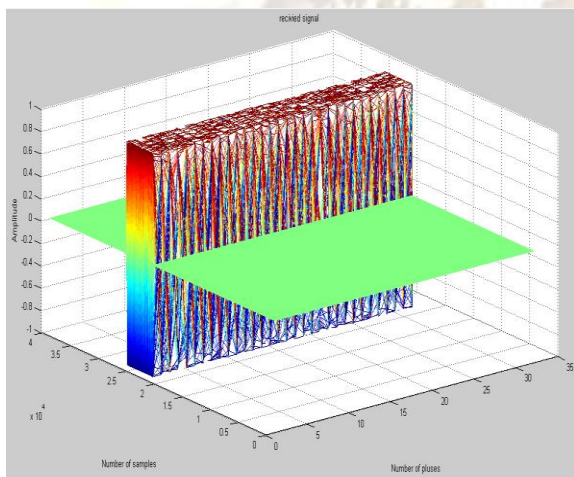


Figure 8 : Received echo signal from the target containing 32 pulses.

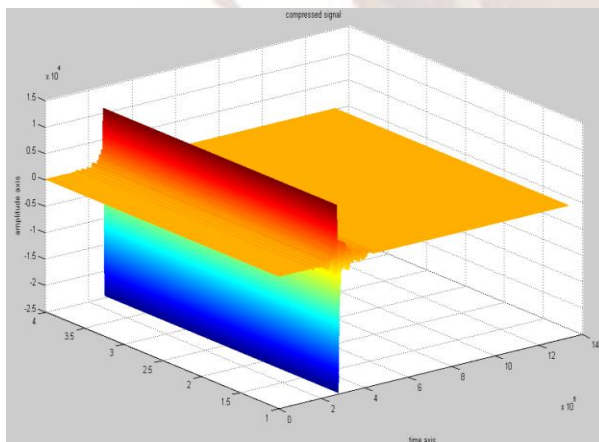


Figure 9 : Resultant signal after applying matched filter and cross correlation function, (compressed signal).

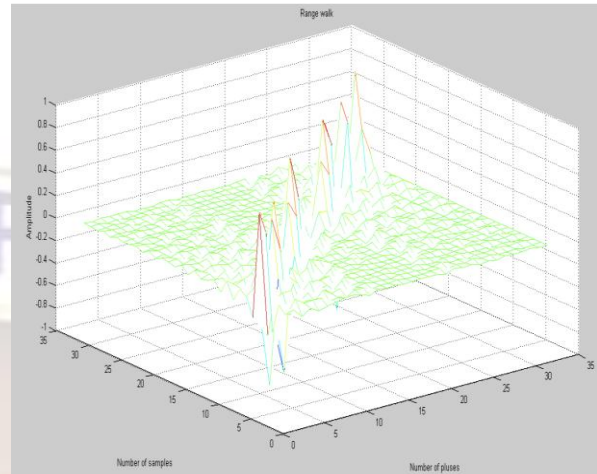


Figure 10: Range walk problem due to target high velocity and acceleration.

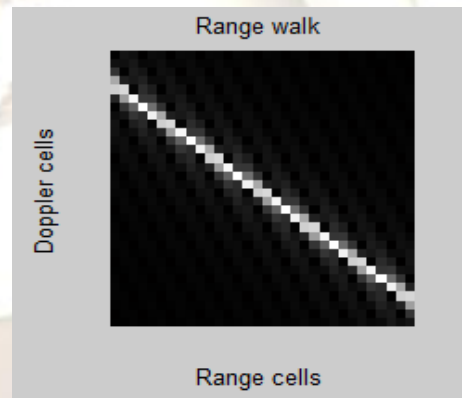


Figure 11 : Spectral spreading of single target due to range walk.

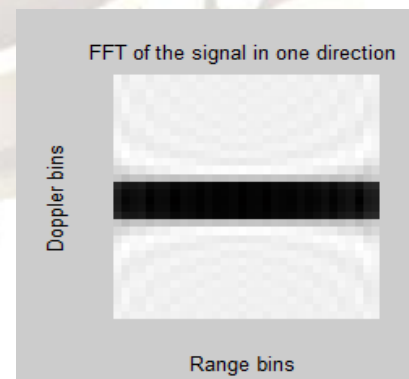


Figure 12 : FFT of the signal with respect to the fast time axis.

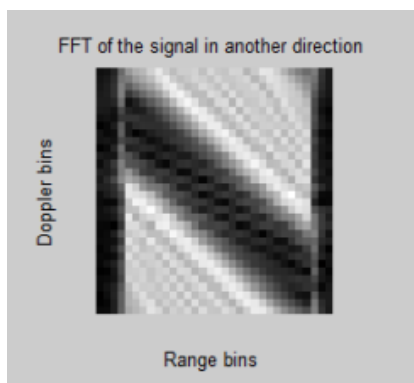


Figure 13 : FFT of the signal with respect to the slow time axis.

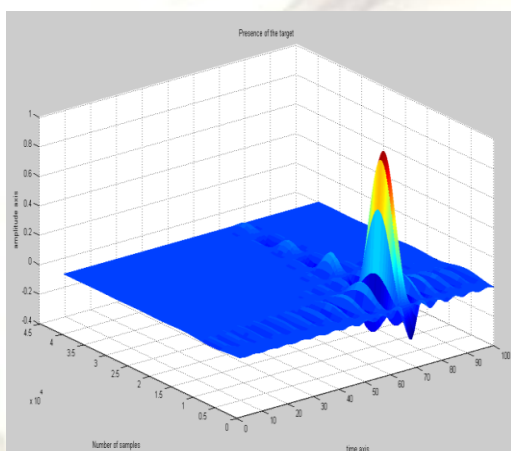


Figure 14: Single target detected

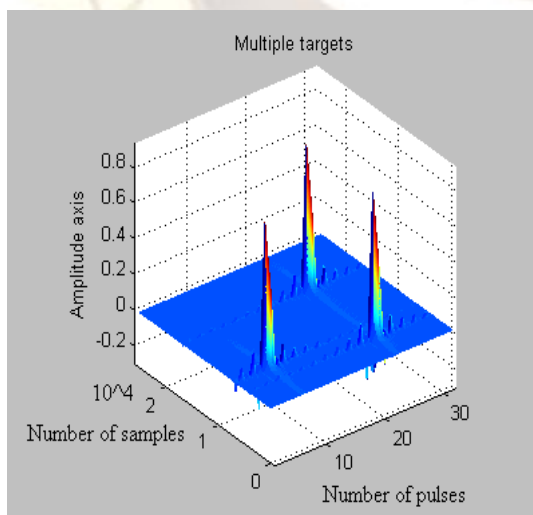


Figure 15: Detection of multiple targets

This detection of the targets are after applying the range walk compensation method as explained above and spatial-temporal cell averaging CFAR algorithm which sets the threshold value for clear target detection against the heavy clutter and noisy background.

VII. CONCLUSION

For targets with high velocity, range walk always happens and creates difficulties for target detection. An efficient and accurate method combining the digital match filtering with compensation processing is put forward. This method compensates the envelope migration by shifting the matching weight coefficients. Also the combined method of spatial and temporal CFAR was introduced to benefit from their advantages at the same time. By using this method, the target can be detected more accurately in heavy clutter and noisy environment.

ACKNOWLEDGMENT

The authors express their gratitude to the management of KL University and the Department of Electronics and Communication Engineering for their endorsement during this work.

REFERENCES

- [1] Zhang, S. S., Zeng, T., Long, T., and Yuan, H. P. Dim target detection based on keystone transform. In *Proceedings of the IEEE International Radar Conference*, May 2005, 889—894.
- [2] Wang, J., Zhang, S. H., and Bao, Z. On motion compensation for weak radar reflected signal detection. In *The 6th International Conference on Signal Processing*, vol. 1, Aug. 2002, 1445—1448.
- [3] Chen, J. J., Chen, J., and Wang, S. L. Detection of ultra-high speed moving target based on matched Fourier transform. In *Proceedings of the CIE International Conference on Radar*, Oct. 2006, 1—4.
- [4] So, H. C., Ma, W. K., and Chan, Y. T. Detection of narrowband random signals via spectrum matching. In *Midwest Symposium on Circuits and Systems*, Aug. 1998, 238—241.
- [5] Wang, Z., Willett, P., and Streit, R. Detection of long-duration narrowband processes. *IEEE Transactions on Aerospace and Electronic Systems*, **38**, 1 (Jan. 2002), 211—227.
- [6] Sadler, B. M., Giannakis, G. B., and Lii, K-S. Estimation and detection in non-Gaussian noise using higher order statistics. *IEEE Transactions*

- on *Signal Processing*, **42**, 10 (Oct. 1994), 2729—2741.
- [7] Hock, K. M. Narrowband weak signal detection by higher order spectrum. *IEEE Transactions on Signal Processing*, **44**, 4 (Apr. 1996), 874—879.
- [8] Garth, L. M. and Bresler, Y. The degradation of higher order spectral detection using narrowband processing. *IEEE Transactions on Signal Processing*, **45**, 7 (July 1997), 1770—1784.
- [9] Tsao, J., Shyu, W. J., and Mar, J. Detection of narrowband signals by Gabor's expansion of spectrum. In *Proceedings of the International Conference on Acoustics, Speech, and Signal Processing*, vol. 5, Apr. 1991, 3201—3204.
- [10] Willett, P., Wang, Z., and Streit, R. Wavelets in the frequency domain for narrowband process detection. In *Proceedings of the IEEE International Conference on Acoustics, Speech, and Signal Processing*, vol. 5, May 2001, 3193—3196.
- [11] Kim, I. J., Park, S. R., Song, I., Lee, J., Kwon, H., and Yoon, S. Detection schemes for weak signals in first-order moving average of impulsive noise. *IEEE Transactions on Vehicular Technology*, **56**, 1 (Jan. 2007), 126—133.
- [12] Sharif, M. R. and Abeysekera, S. S. Efficient wideband signal parameter estimation using a Radon-ambiguity transform slice. *IEEE Transactions on Aerospace and Electronic Systems*, **43**, 2 (Apr. 2007), 673—688.
- [13] Sharif, M. R. and Abeysekera, S. S. Efficient wideband sonar parameter estimation using a single slice of Radon-ambiguity transform. In *Proceedings of the IEEE International Conference on Acoustics, Speech, and Signal Processing*, vol. 5, Mar. 2005, 605—608.
- [14] Fu, Z., Yin, Z. P., Zhang, D. C., and Chen, W. D. Modified motion parameter estimation for space object imaging. In *Proceedings of the International Conference on Microwave and Millimeter Wave Technology*, vol. 4, Apr. 2008, 2043—2046.
- [15] Kelly, E. J. and Wishner, R. P. Matched-filter theory for high-velocity, accelerating targets. *IEEE Transactions on Military Electronics*, **MIL-9**, 1 (Jan. 1965), 56—69.
- [16] Berizzi, F. and Corsini, G. Autofocusing of inverse synthetic aperture radar images using contrast optimization. *IEEE Transactions on Aerospace and Electronic Systems*, **32**,3(July1996),1185—1191.
- [17] P. Ramesh Babu and R. Prasanthi, "Analysis of CFAR Techniques and FPGA Realization for Radar Detection," *Proceedings of International Conference on Intelligent Knowledge Systems*, 2004.
- [18] M.I Skolnik, *RADAR Handbook*, McGraw-Hill, 1990.
- [19] PICCARDI, M., Background subtraction techniques: a review. In *Proceedings of International Conference on Systems, Man and Cybernetics*. The Hague, The Netherlands, October 2004.